arXiv:0810.3745v3 [astro-ph] 24 Oct 2008

X-ray studies of HESS J1837–069 with Suzaku and ASCA: a VHE γ-ray source originated from the pulsar wind nebula

Takayasu ANADA, Ken EBISAWA, Tadayasu DOTANI, and Aya BAMBA

Institute of Space and Astronautical Science, JAXA, 3-1-1 Yoshinodai, Sagamihara, Kanagawa 229-8510

anada@astro.isas.jaxa.jp, ebisawa@astro.isas.jaxa.jp, dotani@astro.isas.jaxa.jp, bamba@astro.isas.jaxa.jp

(Received 2008 August 29; accepted 2008 October 15)

Abstract

We present the ASCA and Suzaku studies of the TeV source HESS J1837–069, which has not been identified in other wave-lengths. We confirm the presence of two X-ray sources in the Suzaku XIS image, AX J1838.0–0655 and AX J1837.3–0652, near both ends of the elongated TeV emission region. The XIS spectra of the two sources are reproduced by an absorbed power-law model, whose parameters are all consistent with those determined by the ASCA data. Recently, 70.5 ms X-ray pulsation has been detected with RXTE in the sky region including HESS J1837–069 (2008, ApJ, 681, 515). Using the ASCA GIS data which has both timing and imaging capabilities, we identified the pulsation source as AX J1838.0–0655. The pulse periods determined by ASCA and Suzaku, and that reported with RXTE indicate steady spin-down at $\dot{P} = 4.917(4) \times 10^{-14}$ s s^{-1}. These results suggest that AX J1838.0–0655 is an intrinsically stable source, and presumably a pulsar wind nebula (PWN). We discuss the possibility that AX J1838.0–0655 is associated with HESS J1837–069 and the VHE γ-ray emission is originated from the PWN.

Key words: ISM: individual (HESS J1837–069) — stars: neutron — X-rays: individual (AX J1838.0–0655, AX J1837.3–0652)

1. Introduction

Galactic plane survey with the H.E.S.S. Cherenkov telescope system revealed the presence of dozens of new very-high-energy (VHE) γ-ray sources (Aharonian et al. 2005; Aharonian et al. 2006). Many of them have no counterparts in other wave-lengths, and are thus called

"unidentified (unID) TeV sources". Today, there are about 40 such unidentified TeV sources on the Galactic plane (Hinton 2007). Most of them are located within 1 degree from the Galactic plane, and some are intrinsically extended. Some of them are suspected to be pulsar wind nebulae (PWNe) or supernova remnants (SNRs)(Hinton 2007), but origins of most sources are still unclear.

HESS J1837–069 is one of the VHE γ-ray sources discovered by the Galactic survey with H.E.S.S. in 2004 centering at the position of (RA, Dec) = ($18^{\rm h}37^{\rm m}42\overset{\rm s}{.}7$, $-6^\circ55'39''$). It has a significantly elongated shape with an extension of $7'\times3'$ (Aharonian et al. 2005; Aharonian et al. 2006). No X-ray sources are known to be positionally coincident to the center of HESS J1837–069, although AX J1838.0–0655, which is located at the Galactic south edge of the HESS source, was suggested to be a possible counterpart (Gotthelf & Halpern 2008). ASCA observation revealed that AX J1838.0–0655 has very hard and strongly absorbed spectrum (Bamba et al. 2003). INTEGRAL (Malizia et al. 2005) observations also support this result. Recently, Gotthelf & Halpern (2008) discovered a 70.5 ms pulsation with RXTE in the sky field including AX J1838.0–0655, and also resolved a bright point source surrounded by diffuse emission with Chandra. They concluded that AX J1838.0–0655 is a PWN. Here we report the results of ASCA archival data analysis and the newly obtained Suzaku observation of HESS J1837–069/AX J1838.0–0655.

2. Observation

We observed HESS J1837–069 with Suzaku (Mitsuda et al. 2007) in March, 2007. Suzaku is equipped with two types of the instruments: the X-ray Imaging Spectrometer (XIS: Koyama et al. 2007) at the focal plane of X-Ray Telescope (XRT: Serlemitsos et al. 2007) and the Hard X-ray Detector (HXD: Takahashi et al. 2007, Kokubun et al. 2007), which is non-imaging instrument with a $34'\times34'$ full-width half-maximum (FWHM) square field-of-view (FOV) below $\sim$ 100 keV. The observation was carried out with the HXD optical axis (which is $\sim 3'$ offset of that of XIS) placed at the center of HESS J1837–069 in order to optimize the HXD throughput. Three XISs (XIS 0, 1, 3) were operated in the normal clocking mode with Spaced-row Charge Injection (SCI) (Nakajima et al. 2008). We analyzed the data prepared by the version 2.0 pipeline. We applied the standard screening criteria to both the XIS[1] and HXD[2] data to obtain cleaned event lists. After the data screening, the net exposures were 42.2 ks and 37.7 ks for XIS and HXD, respectively.

We also used the same ASCA archival data in the current study, that were previously published by Bamba et al. (2003). HESS J1837–069 was in the FOV of ASCA GIS in both the 1997 and 1999 observations (Bamba et al. 2003). The data was screened based on the same

[1] http://www.astro.isas.jaxa.jp/suzaku/process/v2changes/criteria_xis.html

[2] http://www.astro.isas.jaxa.jp/suzaku/process/v2changes/criteria_hxd.html

Table 1. Journal of the ASCA/Suzaku observations of HESS J1837–069

Satellite	Sequence ID	Start time (UT)	End time (UT)	Aim point (J2000)		Net exposure
		(yyyy/mm/dd hh:mm)		R.A.	Decl.	(ks)
ASCA	55002090	1997/10/14 09:12	1997/10/14 14:17	$18^{\rm h}37^{\rm m}48\overset{\rm s}{.}0$	$-6°36'42''$	12.4* / 8.4†
ASCA	57029000	1999/09/26 18:12	1999/09/28 03:30	$18^{\rm h}37^{\rm m}45\overset{\rm s}{.}6$	$-6°36'45''$	37.3* / 17.6†
Suzaku	401026010	2007/03/05 12:49	2007/03/06 10:17	$18^{\rm h}37^{\rm m}42\overset{\rm s}{.}7$	$-6°55'39''$	42.2‡ / 37.7§

* GIS, high and medium bit-rate data

† GIS, high bit-rate data only

‡ XIS

§ HXD-PIN

Table 2. Suzaku detected X-ray sources in the vicinity of HESS J1837–069

Src	coordinate* (J2000)		Association
	R.A.	Decl.	
1	$18^{\rm h}38^{\rm m}03^{\rm s}$	$06°55'43''$	AX J1838.0–0655
2	$18^{\rm h}37^{\rm m}21^{\rm s}$	$06°53'14''$	AX J1837.3–0652

* Error radius (90%) is $19''$ (Uchiyama et al. 2008)

criteria as Bamba et al. (2003).

The net exposures after screening are summarized in table 1 with the journal of Suzaku and ASCA observations. We used HEADAS version 6.3.1 software package for all the data analysis in the present paper.

3. Results

3.1. X-ray Image

We extracted the XIS image in 0.4–10.0 keV for each sensor. The data between 5.73–6.67 keV were removed from the image to exclude the calibration sources. We corrected the vignetting effect by dividing the image with the flat sky image simulated at 4.0 keV using the XRT+XIS simulator `xissim` (Ishisaki et al. 2007). The image was binned to 8×8 pixels and smoothed with a Gaussian function of $\sigma = 0\overset{\prime}{.}42$. Combined Suzaku XIS (0+1+3) image is shown in figure 1. Two X-ray sources are seen at the edges of galactic south and north of HESS J1837–069. Hereafter, we refer the two sources as Src 1 and Src 2 in this paper as indicated in figure 1. We determined the peak positions of Src 1 and Src 2 as listed in table 2. These positions are consistent with those of the ASCA sources, AX J1838.0–0655 and AX J1837.3–0652, respectively. Locations of these two sources are significantly offset from the center of HESS J1837–069 ($6\overset{\prime}{.}4$ for Src 1 and $5\overset{\prime}{.}7$ for Src 2), although they are both spatially compatible with the reported extension of HESS J1837–069.

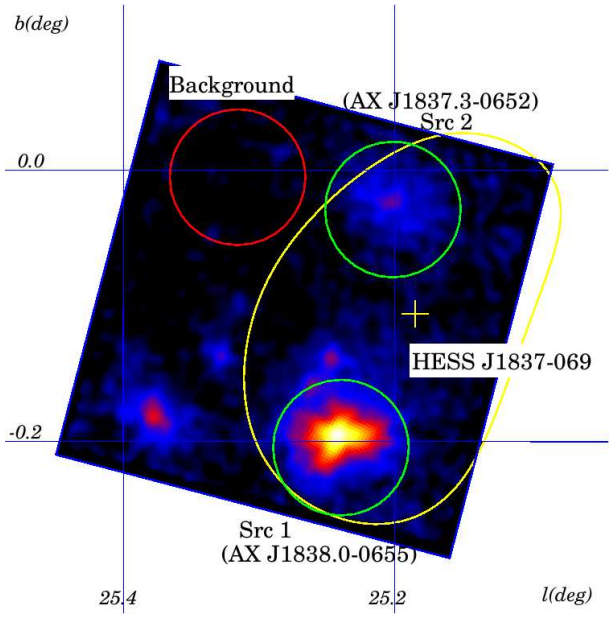

Fig. 1. Suzaku XIS (0+1+3) image in Galactic coordinate around HESS J1837–069 in the 0.4-10.0 keV band. The data between 5.73–6.67 keV were filtered out to remove the calibration sources. The pseudo-color represents vignetting-corrected, log-scaled intensity levels. Yellow line represents the $e^{-1/2}$ contour to the peak of the VHE γ-ray image of HESS J1837–069[3] (Aharonian et al. 2006). Two sources in the green circles are referred to Src 1 (AX J1838.0–0655) and Src 2 (AX J1837.3–0652). Background data were extracted from the red circle whose vignetting is almost the same as the two sources. All the radii of the circles are $3'$. 2E1835.5-0650 was also detected at the position of $(l, b) = (25.^{\circ}38, -0.^{\circ}18)$.

3.2. Energy Spectra

We extracted the energy spectra of Src 1 and Src 2 within the $3'$ circular regions centered on the sources to avoid nearby faint point source detected by Chandra, which enclose $\sim$90% of photons for each point source (green circles in figure 1). Background data were extracted from the source-free region as indicated by a red circle in figure 1, whose vignetting is almost same as that of Src 1 and Src 2. Figure 2 shows the XIS spectra (averaged for XIS 0, 1 and 3) of Src 1 and Src 2 in the 0.4–10 keV band. The 1.7–2.0 keV band was ignored from the analysis because of large calibration uncertainties around the Si edge[4]. We generated detector and auxiliary response files using `xisrmfgen` and `xissimarfgen` for each source (Ishisaki et al. 2007). We fitted the spectra with an absorbed power-law model using XSPEC version 12.3.1. The fit results are summarized in table 3.

We also reanalyzed the data obtained with ASCA GIS in 1997 and 1999 to determined the errors of the source fluxes, which are not published in Bamba et al. (2003). We extracted the data of Src 1 and Src 2 in the 0.7–10 keV band from the same regions as Bamba et al. (2003)

[3] Fits file is available from http://www.mpi-hd.mpg.de/hfm/HESS/public/publications/ApJ_636.html

[4] http://www.astro.isas.jaxa.jp/suzaku/doc/suzaku_td/

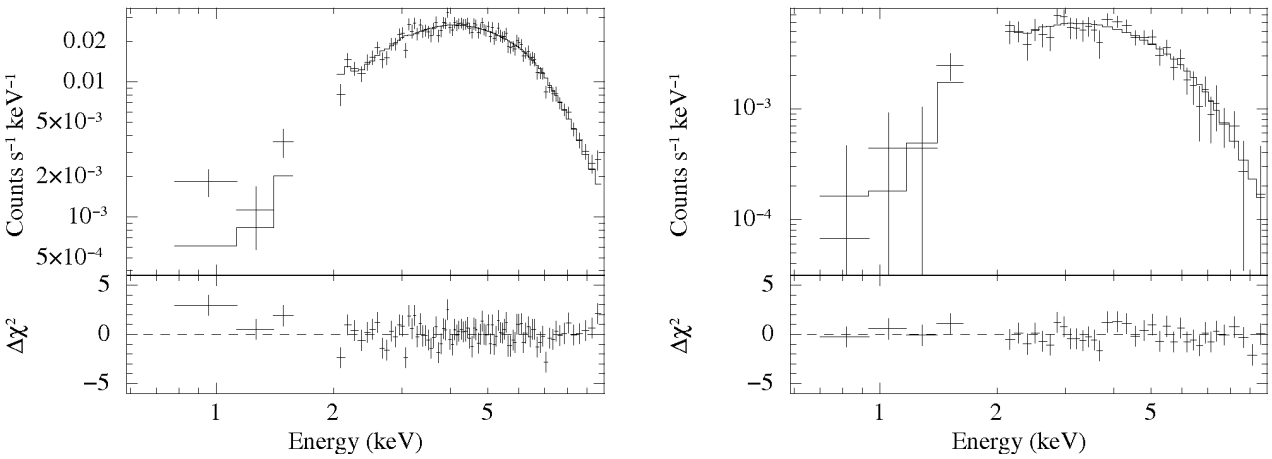

Fig. 2. Background-subtracted XIS spectra of Src 1 (left) and Src 2 (right), respectively. Solid lines show the best-fit model. The bottom panels show residuals to the best-fit model.

Table 3. Best-fit parameters of the absorbed power-law model

Source	Instrument	Γ	$N_{\rm H}{}^*$	Flux†	χ^2 / dof
1	Suzaku/XIS	1.27±0.11	5.4±0.5	$13.2^{+0.8}_{-0.6}$	97.7 / 86
	ASCA/GIS	0.8±0.4	$4.0^{+1.6}_{-1.3}$	14^{+2}_{-1}	12.9 / 12
2	Suzaku/XIS	$2.2^{+0.4}_{-0.3}$	$4.6^{+1.5}_{-1.0}$	$3.1^{+1.5}_{-0.7}$	27.1 / 37
	ASCA/GIS	$2.4^{+0.9}_{-0.8}$	$6.2^{+3.4}_{-2.2}$	6^{+13}_{-3}	35.6 / 33

Note. — Errors represent single-parameter 90% confidence limit.

* Absorption column density using the solar abundance ratio (Anders & Ebihara 1982) in the unit of 10^{22} cm^{-2}.

† Unabsorbed flux in the 0.7-10.0 keV band in the unit of 10^{-12} ergs cm^{-2} s^{-1}.

and subtracted the background extracted from the source-free regions near the sources. We summed up the data in 1997 and 1999 to improve statistics as was done by Bamba et al. (2003). We fitted the spectra with an absorbed power-law model and calculated the single-parameter 90% confidence regions of the unabsorbed fluxes. The results are listed in table 3.

3.3. Timing Analysis

Because X-ray pulsation was recently detected from the sky region including HESS J1837–069 (Gotthelf & Halpern 2008), we carried out timing analysis of the Suzaku HXD-PIN and ASCA GIS data to study the long-term change of the pulse period and to identify the source of pulsation. Although HXD-PIN has a large FOV, there are no significant contamination sources to Src 1 in its FOV. Thus we searched for pulsation with HXD-PIN. When we analyzed the HXD-PIN data, we carefully examined the best energy range to maximize the signal-to-noise ratio. In order to minimize the contribution of non-X-ray background (NXB)[5] , cosmic X-ray

[5] We used the quick-version of the NXB model explained in SUZAKUMEMO-2008-03 (http://www.astro.isas.jaxa.jp/suzaku/doc/suzakumemo/suzakumemo-2008-03.pdf), and also in Fukazawa

background (CXB) and Galactic ridge X-ray emission (GRXE), we selected 12–23 keV for the analysis of the PIN data. In this energy band, the source count rate was 0.41 counts s^{-1} whereas the count rates of NXB and CXB+GRXE were 0.32 and 0.04 counts s^{-1}, respectively. We then applied barycentric correction to the PIN data using `aebarycen` (Terada et al. 2008). Using the `efsearch` ftool, we searched for pulsation at 128 trial periods between 0.0704949–0.0704987 sec and found a significant peak at 0.07049672(8) s with $\chi^2 \sim 46$ (9 degrees of freedom). Here the 1σ error is indicated in parentheses, which was calculated according to Larsson (1996). The chance probability to obtain such a large χ^2 in 128 trial is only 0.01%.

Whereas HXD-PIN is a non-imaging instrument, GIS has an imaging capability and can extract the events from the source region. Assuming that the pulsation originates from Src 1, we searched the GIS data of Src 1 for pulsation. Although the nominal time resolution of GIS in the PH mode is 62.5 ms in the high telemetry bit rate (Ohashi et al. 1996), we can achieve higher time resolution up to 4 ms when the total count rate is low. The GIS event data were output to the fixed format telemetry, whose relative location within a 62.5 ms slot was designed to indicate the finer timing information[6]. The photon arrival time of GIS in the ASCA archive is all assigned taking this finer timing information into account. Because Src 1 (and other sources in the GIS FOV) is dim (2.3 counts s^{-1} compared to the telemetry capacity of 128 counts s^{-1}), we can fully utilize the higher than the nominal time resolution of GIS. The GIS image of Src 1 was elongated due to the proximity to the edge of the FOV. Thus we used an elliptical region of $1\farcm7 \times 0\farcm9$ to extract the source events. We used only the high bit rate data in 1999, and 224 photons in 2–10 keV (including background) was extracted in total. We applied barycentric correction using `timeconv`. We searched for pulsation at 128 trial periods between 0.0704838–0.0704865 sec and found a significant peak at 0.070485(2) sec with $\chi^2 \sim 38$ (9 degrees of freedom). The chance probability to obtain a χ^2 larger than 38 is only 0.2%. Thus the peak is statistically significant.

We show the folded pulse profiles of PIN and GIS in figure 3 with respective pulse periods determined above. Parameters determined by the timing analysis above are summarized in table 4. We divided the PIN data into two phases: on-peak (phase 0.65–1.05) and off-peak (phase 0.05-0.65). We extracted the pulsed spectrum by subtracting the off-peak spectrum from the on-peak spectrum, and fitted it with a power-law model in the 12–50 keV band. The fitted spectrum is shown in figure 4. Best-fit photon index and the flux in the 12–50 keV band were found to be $\Gamma = 2.0^{+1.0}_{-0.9}$ and $F = 1.8^{+0.8}_{-0.6} \times 10^{-11}$ ergs cm^{-2} s^{-1}. We tried the same analysis for the GIS data, but could not obtain a meaningful result due to poor statistics.

et al. (2009).

[6] http://heasarc.gsfc.nasa.gov/docs/asca/newsletters/time_assignment4.html

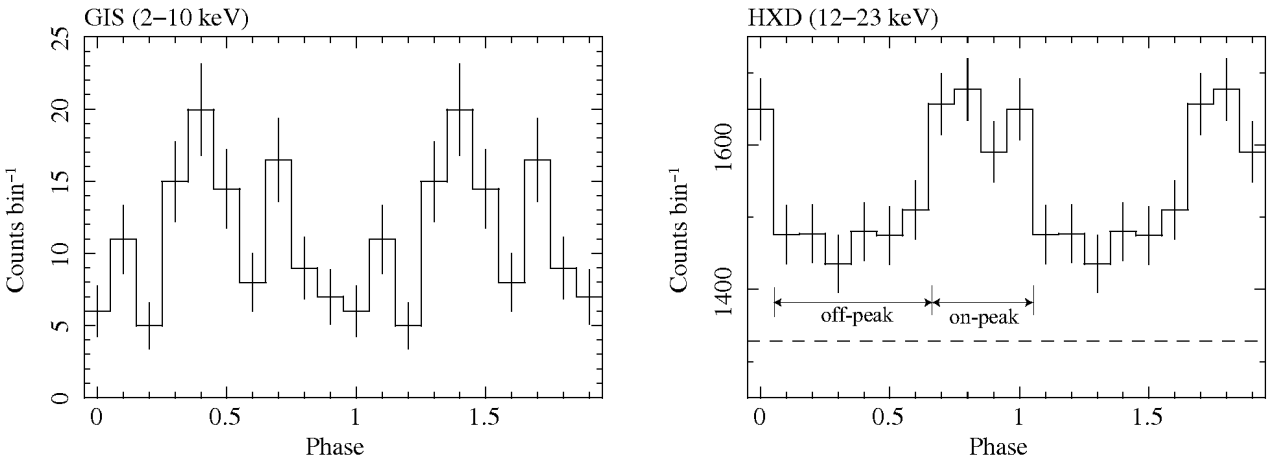

Fig. 3. Left: Pulse profile obtained with the GIS data of Src 1 in the 2–10 keV band. Right: Pulse profile obtained with PIN in the 12–23 keV band. Dashed line indicates the estimated count rate of the background. The pulse profile is corrected for the constant dead time (93%).

Table 4. Timing Parameters of Src 1

Parameter	GIS	HXD-PIN
Epoch (MJD TDB)	51447	54164
Period, P (ms)	70.485(2)	70.49672(8)

Note. — 1σ uncertainties are given in parentheses.

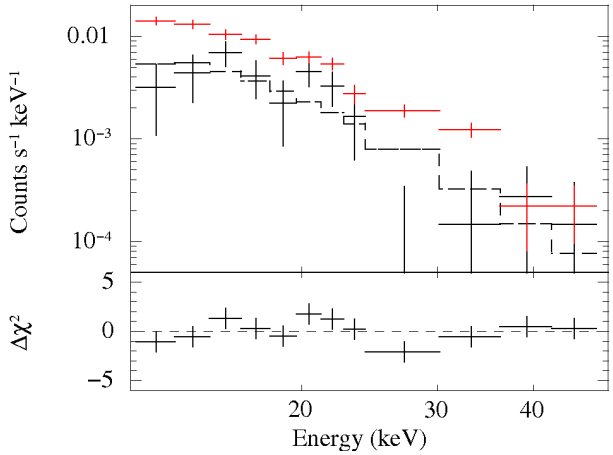

Fig. 4. Black line represents HXD-PIN pulsed spectrum obtained by subtracting the off-peak spectrum from the on-peak spectrum. Dashed histogram represents the best-fit power-law model. Total HXD-PIN spectrum subtracted NXB is also shown as red line.

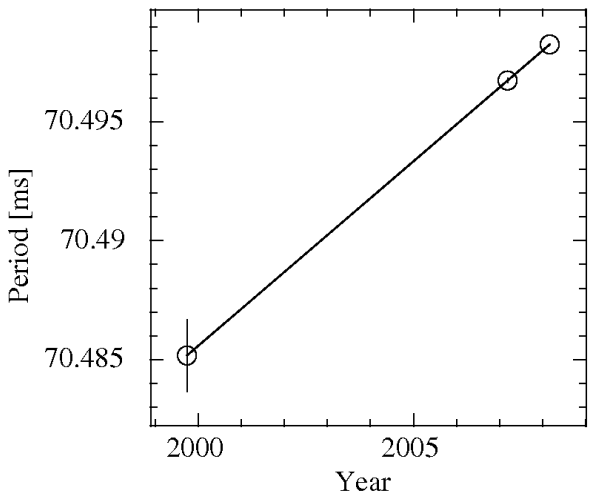

Fig. 5. History of the pulse period. The data points from left to right indicate the pulse periods determined by ASCA, Suzaku and RXTE, respectively.

4. Discussion

4.1. Nature of Src 1

We have confirmed that the source of 70.5 ms pulsation, which was recently discovered by RXTE, is indeed Src 1. The pulse profiles obtained by GIS and HXD-PIN are consistent with that of RXTE. We show in figure 5 a long-term history of the pulse period. All the data are consistent with the stable spin-down with $\dot{P} = 4.917(4) \times 10^{-14}$ s s^{-1} (1σ error is indicated in parentheses), which is also consistent with the instantaneous spin-down rate determined by RXTE for the interval of $\sim$ 16 days (Gotthelf & Halpern 2008). The spectral parameters (flux, photon index, column density) of Src 1 determined by the GIS data were all consistent with those of XIS. The flux and the column density were also consistent with those of Chandra. Therefore, we conclude that Src 1 is an intrinsically stable source.

Gotthelf & Halpern (2008) claimed that the Chandra spectrum of the pulsar component was significantly harder ($\Gamma = 0.5 \pm 0.2$) than the pulsed component obtained by RXTE in 2–20 keV ($\Gamma = 1.2 \pm 0.1$). They suggested a steepening of the spectrum in the 8–15 keV band. The Suzaku HXD-PIN data indicate a photon index of $\Gamma = 2.0^{+1.0}_{-0.9}$ for the pulsed component in the 12–50 keV. This photon index is consistent with the RXTE result and supports the steepening of the spectrum in the hard X-ray band.

4.2. Nature of Src 2

Src 2 was also observed by ASCA and is known to have a non-thermal spectrum (Bamba et al. 2003). Current Suzaku observation suggests no time variation of Src 2 since the ASCA observation. Therefore we speculate that Src 2 is also a PWN. However, Chandra could detect neither the putative pulsar point source in Src 2 nor any pulsation (Gotthelf & Halpern 2008).

Further observations are required to reveal the nature of this source.

4.3. Origin of HESS J1837–069

Because Src 1 is slightly offset from the center of HESS J1837–069, we need to check the chance coincidence of the sources. The chance probability for high-power pulsars and VHE γ-ray sources was estimated by Carrigan et al. (2007). For Src 1 with $\dot{E}/d^2 \sim 10^{35}$ ergs s^{-1} kpc^{-2}, the chance probability is $\sim 12\%$. Thus we consider Src 1 is likely to be associated to HESS J1837–069.

We thank Gerd Pühlhofer and Stefan Wagner for providing the HESS image FITS file of HESS J1837–069. We also thank Ryo Yamazaki for his valuable comment on the discussion. This work made use of archival data of ASCA from Data Archives and Transmission System (DARTS) maintained by C-SODA at JAXA/ISAS. This work was partially supported in part by Grant-in-Aid for Scientific Research of the Japanese Ministry of Education, Culture, Sports, Science and Technology, No. 19·4014 (A. B.).

References

Aharonian, F., et al. 2005, Science, 307, 1938
Aharonian, F., et al. 2006, ApJ, 636, 777
Anders, E., & Ebihara, M. 1982, Geochim. Cosmochim. Acta, 46, 2363
Bamba, A., Ueno, M., Koyama, K., & Yamauchi, S. 2003, ApJ, 589, 253
Carrigan, S., Hinton, J. A., Hofmann, W., Kosack, K., Lohse, T., Reimer, O., & for the H. E. S. S. Collaboration 2007, arXiv:0709.4094
Fukazawa, Y., et al. submitted to PASJ, 2009
Gotthelf, E. V., & Halpern, J. P. 2008, ApJ, 681, 515
Hinton, J. 2007, ArXiv e-prints, 712, arXiv:0712.3352
Ishisaki, Y., et al. 2007, PASJ, 59, 113
Kokubun, M., et al. 2007, PASJ, 59, 53
Koyama, K., et al. 2007, PASJ, 59, 23
Larsson, S. 1996, A&AS, 117, 197
Malizia, A., et al. 2005, ApJL, 630, L157
Mitsuda, K., et al. 2007, PASJ, 59, 1
Morrison, R., & McCammon, D. 1983, ApJ, 270, 119
Nakajima, H., et al. 2008, PASJ, 60, 1
Ohashi, T., et al. 1996, PASJ, 48, 157
Serlemitsos, P. J., et al. 2007, PASJ, 59, 9
Takahashi, T., et al. 2007, PASJ, 59, 35
Terada, Y., et al. 2008, PASJ, 60, 25
Uchiyama, Y., et al. 2008, PASJ, 60, 35

This figure "hessj1837.jpg" is available in "jpg" format from:

http://arXiv.org/ps/0810.3745v3